

Geomorphic and structural assessment of active tectonics in NW Alborz

Bitá Javidfakhr^{1*}, Seiran Ahmadian²

¹ Department of Geology, University of Zanjan, Iran

² (Cape Consulting Group) N 303, Motahari Avenue, Tehran, Iran

*Corresponding author, e-mail: bjavid@znu.ac.ir

(received: 29/01/2018 ; accepted: 20/06/2018)

Abstract

Alborz Mountains is a region of active deformation within Arabia-Eurasia collision zone. The study fault system in western Alborz comprises abundant evidence of active faulting accompanied by occurrence of historical earthquakes. Active tectonics of Manjil-Rudbar fault zone whose movement caused destructive 1990 Manjil-Rudbar earthquake was concentrated in this article through geomorphic and structural analyses. Major fault segments were mapped in order to recognize structural and geomorphic features of the fault zone. Satellite images were used to improve the visualization of fault traces in order to constrain their geometry considering structural linkage between different fault segments. Faults are supported by field geologic data and kinematic measurements. There are left-lateral strike-slip and oblique reverse movements observed all over the fault zone corresponding to recent fault activities of Rudbar, Manjil, Kelishom and Jirandeh (Kashachal) faults. A more complete catalogue of earthquake focal mechanisms is presented to consider general seismic framework of the region. Fault plane solutions indicate a radial pattern of thrusting in western Alborz. We analyzed drainage offsets and Quaternary alluvial fans along major structures in order to understand precise role of major faults in ongoing deformation processes. Most river offsets along active faults are small (about 100m), while left-lateral displacement of up to 500m is also observed in streams cut along major faults.

Keywords: Earthquake, Alborz, Manjil, Rudbar, Quaternary

Introduction

The Arabia-Eurasia convergence rate is reported to be about 22 mmyr⁻¹ at longitude of Bahrain south of the Persian Gulf (Vernant *et al.*, 2004; Reilinger *et al.*, 2006). The Alborz accommodates the motion between South Caspian Basin (SCB) and Central Iran. Alborz Mountains which belong to the Alpine-Himalayan belt, was folded during Late Alpine orogeny and is tectonically active (e.g. Ritz *et al.*, 2006). Considering active geomorphology of northern Iran is crucial because deformation regime in Alborz Mountains is supported by occurrence of large earthquakes. Seismicity and geomorphology provide constraints on style, rate and kinematics of deformation. We investigated recent faulting geomorphic traces to analyze active deformation. Detailed mapping on satellite images complemented by field surveys facilitated determination of different offsets along major faults.

Active tectonics of Manjil-Rudbar fault zone (Tatar & Hatzfeld, 2009; Berberian & Walker, 2010) was studied due to the existence of several active faults and large-magnitude earthquakes documented in western Alborz (Fig. 1, Table 1). Berberian & Walker (2010) studied Manjil-Rudbar earthquake and its aftershocks together with active faulting of the region. We provided a more detailed

view of active faulting in Manjil-Rudbar fault zone, concentrating on geomorphic and Pliocene-Quaternary geologic evidence. The left-lateral strike-slip offsets for similar fault segments presented in this manuscript are generally more conservative. In this paper, we presented new structural data and updated the earlier results. Historical earthquakes were used to assess the seismic hazard in western Alborz. A more complete catalogue of earthquake focal mechanisms (Fig. 1 and Table 1) is presented to consider general seismic framework of the region.

Geodynamic context

Paleotethys Ocean divided the Eurasian Plate from Central Iran blocks in NE Iran while Neotethys Ocean opened in southern boundary of Central Iran blocks during Permian (e.g. Muttoni *et al.*, 2009). Paleotethys suture zone in NE Iran corresponds to the boundary between eastern extend of Alborz and Kopeh-Dagh mountain ranges. Major subsidence phase in SCB began during Early Oligocene, which led to sealing of structures by thick Oligocene to Quaternary sedimentary sequences of western Kopeh Dagh and consequently major uplift phase within Kopeh Dagh and Alborz mountains (Robert *et al.*, 2014, Ballato *et al.*, 2015). Neo-Tethys

Ocean closed in Late Neogene along Bitilis-Zagros suture zone which actually accommodates right-lateral shear. Major tectonic context of Iran is marked by active convergent regime between Arabian and Eurasian plates (e.g. Allen *et al.*, 2004; Ballato *et al.* 2013). Alborz range is extended in E-W direction, originally as a result of N-S convergence of Central Iran in Late Triassic (Berberian, 1983) and SCB movement toward NW in Pleistocene (Jackson *et al.*, 2002; Ritz *et al.*, 2006). Geodetic studies in Alborz (Djamour *et al.*, 2010, 2011) can better clarify its role in accommodation of Arabia-Eurasia convergence (Madanipour *et al.*, 2013, 2017; Van der Boon *et al.*, 2018).

Seismicity of western Alborz

Iran is one of seismically active regions situated on Alpine-Himalayan earthquake belt. Historical and

instrumental seismic events represent occurrence of severe earthquakes over last few centuries in Alborz range (Aziz Zanjani *et al.*, 2013; Rastgoo *et al.*, 2018). Western Alborz experienced more historical seismicity in comparison to eastern Alborz (Zolfaghari, 2009). Taleghan Fault may have been involved in historical 958 Taleghan-Rey earthquake (Ambraseys & Melville, 1982). Damage distribution of historical Upper Polrud earthquake (Ms~7.2, Berberian, 2014) on August 15, 1485 suggests Kelishom Fault as a possible source (Fig. 2B). Historical Alamutrud earthquake occurred on April 20, 1608 (Ms~7.4, Berberian, 2014) and Alamutrud fault was responsible for this event. We used available documents of historical earthquakes which can clarify activity on major structures for presenting a general view of seismic risk for populated cities of Rudbar, Manjil and Loshan.

Table 1. The earthquake source parameters are presented. All angles are presented in degrees. Fig. 1B represents focal mechanisms based on mentioned seismic data. The ID numbers refer to label of each beach ball presented in Fig. 1B. Reference column refers to earthquake source parameters.

N	Date (mm/dd/yyyy)	Time (GMT)	Lat.	Long.	Depth (km)	Magnitude	Ref.	ID	Nodal Planes		
									Strike	Dip	Slip
1	6/24/1903	16:56:00	37.48	48.96		Ms:5.9	AMB				
2	2/9/1903	5:18:00	36.58	47.65		Ms:5.6	AMB				
3	1/9/1905	6:17:00	37.00	48.68		Ms:6.2	AMB				
4	6/17/1948	14:08:31	36.59	49.44		M:5.5	NOW				
5	4/12/1956	22:34:49	37.33	50.26	30	M:5.5	NOW				
6	11/4/1978	15:22:23	37.43	49.11	15	Mw:6.3	CMT	1	177 000	09 81	087 090
7	5/4/1980	18:35:26	38.08	49.41	15	Mw:6.5	CMT	10	179 001	05 85	088 090
8	7/22/1980	5:17:10	37.15	50.67	30	Mw:5.5	CMT	11	135 310	20 70	095 088
9	12/3/1980	4:26:14	37.09	50.53	16	Mw:5.3	CMT	2	160 281	52 57	136 047
10	8/4/1981	18:35:49	37.90	48.84	25	Mw:5.6	CMT	3	159 032	26 73	040 111
11	6/20/1990	21:00:31	36.95	49.52	15	Mw:7.4	CMT	4	200 300	59 73	160 032
12	6/21/1990	9:02:19	36.51	49.77	15	Mw:5.7	CMT	5	204 351	26 68	121 076
13	6/24/1990	9:45:56	36.08	48.91	15	Mw:5.3	CMT	6	234 138	69 75	-163 -022
14	6/7/1990	19:34:59	37.05	49.48	15	Mw:5.3	CMT	12	094 359	37 86	006 127
15	11/28/1991	17:20:01	36.88	49.33	15	Mw:5.6	CMT	7	219 354	36 63	130 065
16	4/19/2002	13:46:53	36.67	49.74	18	Mw:5.2	CMT	8	183 349	26 64	103 084
17	5/11/2006	20:06:45	37.57	48.86	14	Mw:4.8	CMT	9	188 279	67 88	-002 -157

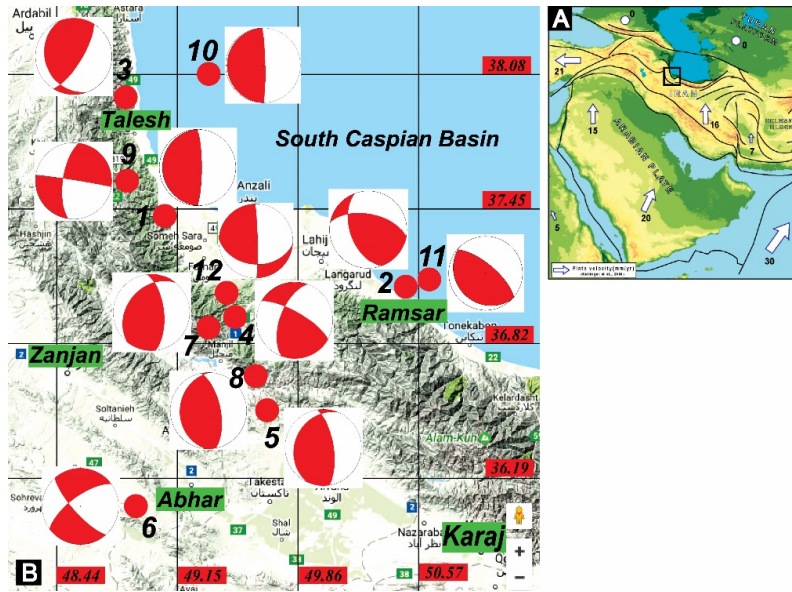


Figure 1. A. Right Figure indicates location of study area in Middle East Alpine collision belt. White arrows and their associated numbers represent velocity vectors in $mmyr^{-1}$ with respect to Eurasia (Reilinger *et al.*, 2006). B. Earthquake fault-plane solutions in SW of south Caspian block is overlain on SRTM data. See Table 1 for details.

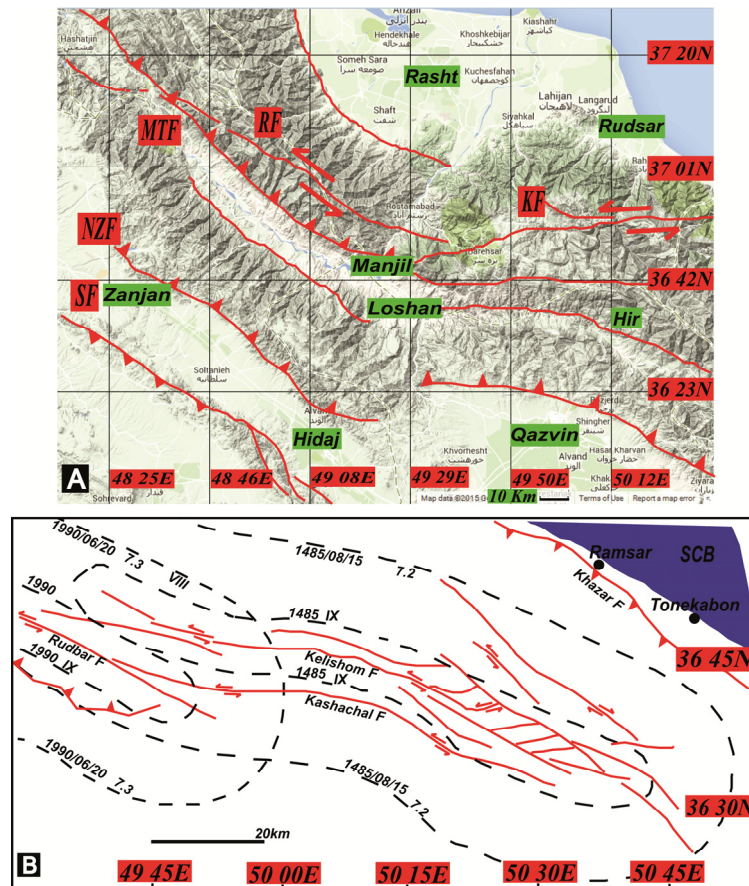


Figure 2. A. Structural map of Manjil-Rudbar fault zone. The abbreviations are as follows: KF. Kelishom fault, MF. Masouleh fault, RF. Rudbar fault, MTF. Manjil thrust fault, NZF. North Zanjan fault, SF. Soltanieh fault and NQF. North Qazvin fault. B. Macroseismicity of historical Upper Polrud earthquake ($M_s \sim 7.2$, Berberian *et al.*, 2014) which happened in 15 August, 1485 along Kelishom left-lateral strike-slip fault.

Soltanieh Fault can probably be responsible for the seismic event in 1803. Furthermore, a terrible earthquake ($M \sim 6.5$ and $I_0 = VII+$) occurred in Qazvin on December 10, 1119 (Ambraseys & Melville, 1982). Firouzabad earthquake on August 16, 1958 had smaller magnitude ($M \sim 6.6$) compared with the last major earthquake in the same area, which occurred on December 13, 1957 ($M \sim 7.1$) (Ambraseys & Moinfar, 1973). Calamitous Manjil-Rudbar earthquake that occurred on June 20, 1990 caused 80km of coseismic range-parallel left-lateral surface ruptures in western Alborz (Berberian & Walker, 2010).

Manjil-Rudbar earthquake (1990)

Manjil-Rudbar earthquake (M_b 6.4, M_s 7.7 and M_w 7.3) occurred on June 20, 1990, in populated areas of northern Iran (Gilan and Zanjan Provinces) along an unknown complex system of reverse faults, later called Baklor-Kabateh-Zardgoli fault. The segments comprise Baklor segment in west, Kabateh segment in center and Zard-Goli segment in east, arranged in a generally WNW trending en-echelon system (Niazi & Bozorgnia, 1992; Hamzehloo *et al.*, 1997; Sarkar *et al.*, 2003; Tatar & Hatzfeld, 2009; Berberian & Walker, 2010). Earthquake rupture dip was reported close to vertical (Berberian & Walker, 2010). The shock was felt in most parts of NW Iran including Arak, Sanandaj and Tabriz. The earthquake completely destroyed 700 villages in Sefidrud river valley (VahidiFard *et al.*, 2017) and in cities of Rudbar, Manjil and Loshan, killing more than 35,000 people. Manjil-Rudbar earthquake had about 50,000 fatalities (National Geophysical Data Center, NOAA, 2016) or 40,000-50,000 casualties (Bastami & Soghrat, 2017). Buildings were destroyed and farms and irrigation channels suffered serious damage (Moinfar & Nader Zadeh, 1990; Berberian *et al.*, 1992; Berberian, 2014).

Earthquake focal analysis indicates left-lateral mechanism for the main shock. Tatar & Hatzfeld (2009) suggested focal mechanisms of different pulses representing a consistent pattern of left-lateral strike-slip fault on a plane striking 295° – 330° and dipping $\sim 78^\circ$ – 99° NE at a depth of ~ 4 – 14 km. Although structural style of the region is dominated by reverse faulting, focal mechanisms of next seismic events (for 11 largest aftershocks M_s 4.6) indicate pure left-lateral strike-slip motion (Gao & Wallace, 1995). Zolfaghari (2009) suggested that strain released during earthquake seems to follow a similar NW trending from similar-magnitude historic

earthquakes of February 23, 958 ($M \sim 7.4$), August 15, 1485 ($M \sim 7.0$) and April 29, 1608 ($M \sim 7.4$).

Geomorphic investigations

Geomorphic studies are important in evaluating earthquake hazards, mostly for areas with recent activity in Holocene and Pliocene-Quaternary (e.g. Kurtz *et al.*, 2018; Sharma *et al.*, 2018). Foothill deposits record climate and tectonic fluctuations which control growth of mountain chains (Audemard, 2003). Landforms such as fault scarps, triangular facets and Quaternary alluvial fans along active fault traces reflect recent tectonic activities. Drainage systems are often influenced by geometry and recent slip of faults in active tectonic regions (Yan & Lin, 2015). Active tectonics of the study region is dominated by NW trending major faults. It is a wide brittle shear zone defined by nearly parallel fault segments. There are systematic patterns of course deflections encountering Manjil-Rudbar fault zone. Geomorphic investigations along Rudbar, Manjil and Kelishom faults provide evidence for left-lateral offsets recorded by streams and alluvial fans, which represent Quaternary activity of faults. Rudbar, Manjil, Kelishom and Kashachal (Jirandeh) faults correspond to a structure located in southern boundary of western Alborz at longitudes between $48.20^\circ E$ and $50.30^\circ E$ (Figs. 1 and 2A).

Kelishom fault zone

Kelishom Fault is a south dipping reverse fault (Fig. 3A) located ~ 10 km from Rudbar fault running for ~ 90 km in western Alborz (Berberian & Walker, 2010). This E-trending high angle reverse fault involves left-lateral strike-slip movements. To west, Kelishom Fault terminates close to Deylaman Fault. Deylaman-Kandovan Fault is one of the major faults in western Alborz (Hakimi Asiabar & Bagheriyan, 2017). Berberian & Walker (2010) suggested eastern part of Kelishom Fault to have a larger component of reverse faulting compared with western segments. Kelishom Fault ruptured during the earthquake on August 15, 1485 representing cumulative left-lateral stream offsets for more than 1km (Berberian & Walker, 2010). Jirandeh (Kashachal) Fault is an E-trending minor left-lateral strike-slip fault running south parallel Kelishom Fault (Fig. 3). Jirandeh Fault trace passes through Jirandeh and Yekonom villages (Fig. 4A). Fig. 4 shows ~ 500 m left-lateral strike-slip movement along Jirandeh Fault. Kelishom and Kashachal faults which run in vicinity of Rudbar Fault are

involved in increasing left-lateral motion rate in Manjil-Rudbar fault zone.

Abbar Fault

Abbar Fault is situated in north of Abbar and is extended parallel with Qezel-Uzan river (Fig. 5A).

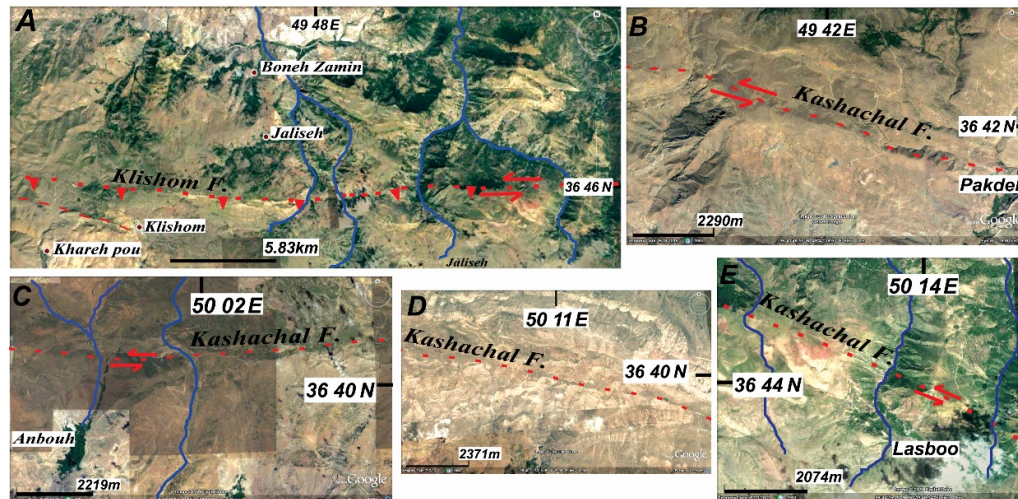


Figure 3. A. Satellite image of Left-lateral strike-slip Kelishom fault passing in north of Kelishom and Khareh Pou villages. B-E. Different segments of left-lateral strike-slip Kashachal (Jirandeh) fault are presented. The rivers are indicative for left-lateral offset.

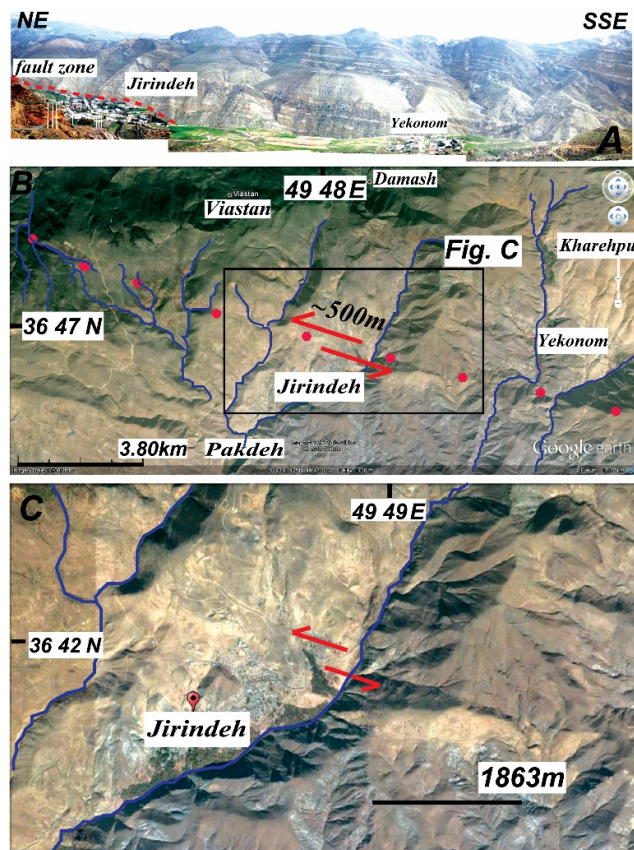


Figure 4. A. Panoramic view of active Jirandeh fault passing Jirandeh and Yekonom villages. B. Left-lateral strike-slip Kelishom fault passing in north of Jirandeh with offsets ~500m considering deflected rivers. C. The rectangle in Fig. B is enlarged here to show the fault trace.

Abbar Fault is a generally NW trending reverse fault with minor left-lateral strike-slip component. This fault has been considered as northwest continuation of Manjil Thrust fault in some previous studies. Left-lateral strike-slip fault affects

Quaternary units in north Chavarzagh (Figs. 5A and 5B) and north Abbar (Fig. 5C). The offset ranges between 130-280m. The fault segments are mostly N to NE dipping and left-lateral offset of ~150m along active Abbar Fault is presented in Fig. 6A.

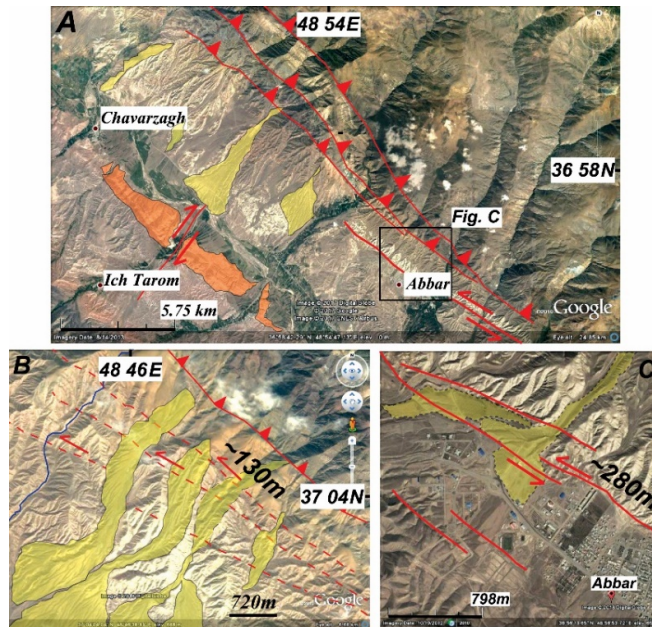


Figure 5. A. Satellite image of Chavarzagh region representing Abbar fault zone. Figs. B and C. Active left-lateral strike-slip fault affecting Quaternary units in north Chavarzagh (Fig. B) and north Abbar (Fig. C). (

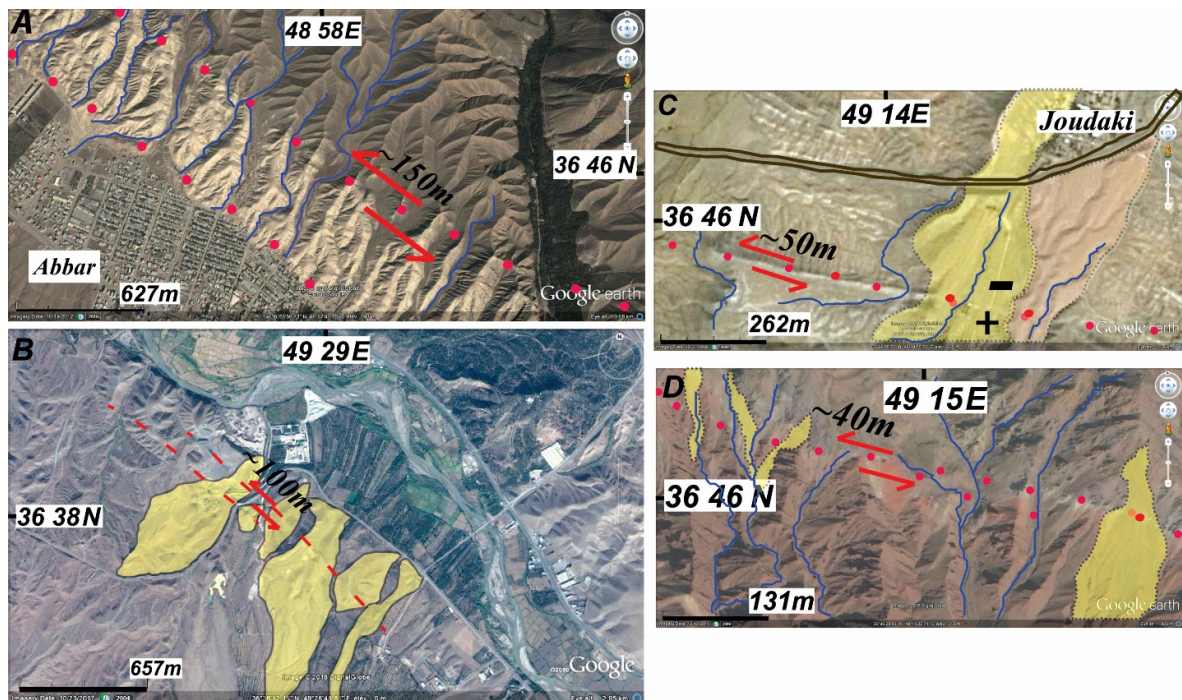


Figure 6. A. Left-lateral offset (~150m) along active Abbar fault. Parallel fault traces are shown by dotted lines. B. Left-lateral offset (~100m) in a fault segment situated in west of Loshan. C and D. Left-lateral offsets along active Manjil fault cutting Quaternary streams and alluvial fans ranging between 40-50m.

Manjil-Rudbar fault zone

Manjil thrust Fault is an active NW trending thrust fault running ~80km in northern parts of Iran. Berberian et al. (1992) suggested reverse slip along fault planes occurred during co-seismic faulting. Different strike-slip fault segments indicate left-lateral offset in the sites situated along Manjil fault zone (Figs. 6 and 7). In west of Loshan, there is a fault segment representing ~100m left-lateral offset considering deflected Quaternary alluvial fans (Fig. 6B). Left-lateral offset of ~40-50m is measured along parallel fault segments in a site situated in vicinity of Joudaki village (Figs. 6C and 6D). Fig. 7A indicates ~120m left-lateral offset situated in SE of Shahveran. Vertical displacement of fault affecting small Quaternary alluvial fan can be observed in Figs. 7A and 7D. WNW trending Rudbar fault is extending in the region for more than 60km from Nusha in southeast toward Rudbar in west. Fault’s dip is north directed. Rudbar Fault has a left-lateral strike-slip mechanism. Permian, Jurassic and Eocene rocks are cut by the fault and can be observed along the fault trace (Nazari & Salamati, 1998). Left-lateral slip rate of 1 mmyr⁻¹ is suggested for Rudbar Fault (Khodaverdian et al., 2015).

Fig. 8A represents nearly parallel reverse faults surrounding a large fold in a site close to Sangrud

village. Major faults are observed in different sites along Manjil fault zone affecting Pliocene-Quaternary deposits (Figs. 8B and 9). The site presented in Fig. 9 is situated in front of Manjil dam. Geologic expression for actual activity of Manjil fault is presented in this image. Displaced river terraces and alluvial fan surfaces (Fig. 10) that occur along Manjil fault suggest that most of Quaternary activity in this structural zone is distributed along Manjil thrust fault trace. Left-lateral strike-slip movement of fault is observed in Quaternary alluvial fans (Figs. 10B and 10D).

Discussion and conclusion

Landslides and rockfalls occurred due to particular geologic and topographic conditions in this region including high rainfall, steep slopes, abrupt topography and narrow valleys. Fatemi Aghda et al. (1992) indicated that most of slope movements are located on or close to active faults. According to Jafari et al. (2000), some other slope instabilities triggered by earthquakes in Alborz region include landslides and rockfalls in Gorgan in 1470 (M 5.5), in Damavand in 1830 (M 7.1), in Talarud in 1935 (M 5.8) and in Bandpey Mazandaran in 1957 (M 6.8). During Manjil-Rudbar earthquake, landslides destroyed a large number of places (Ibrion et al., 2015; Ashtari Jafari, 2016; Bastaminia et al., 2017).

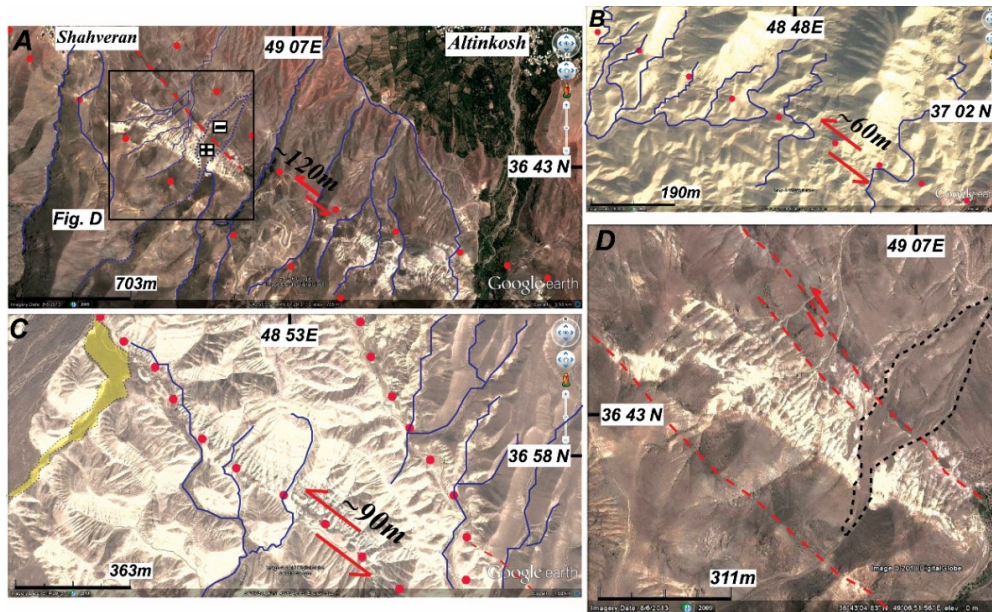


Figure 7. A. Parallel segments of active faults deflecting Quaternary alluvial fans and streams. Horizontal offsets in different splays of faults range between 50m to 120m. B and C. Evidence for left-lateral displacement along active Manjil fault zone through stream channel offsets, ranging from 60m to 90m. The river in western part of image follows the fault line. D. Quaternary alluvial fan in Fig. A is enlarged in this image.

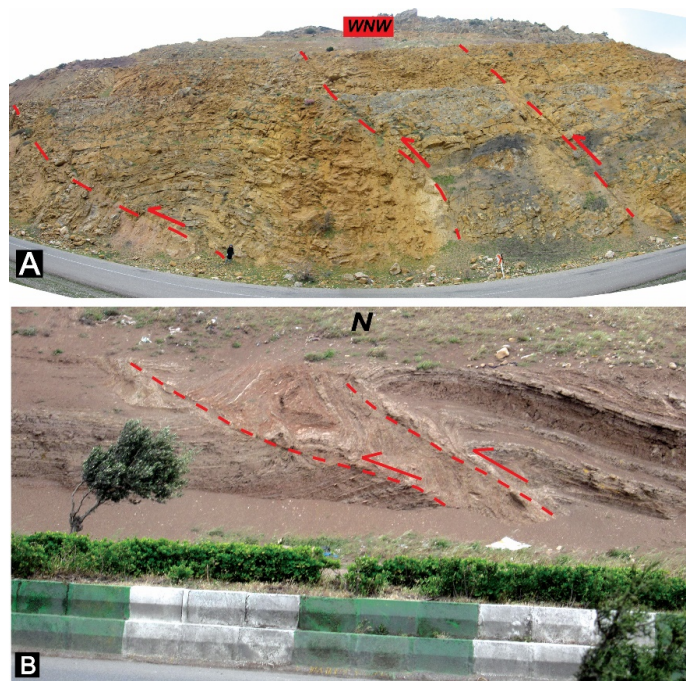


Figure 8. A. Field examples of folding and faulting in vicinity of Sangrud village. There are almost parallel reverse faults surrounding a large fold. B. Manjil thrust fault affecting Quaternary sediments. This site is located beside Manjil Boulevard in vicinity of windy generators.

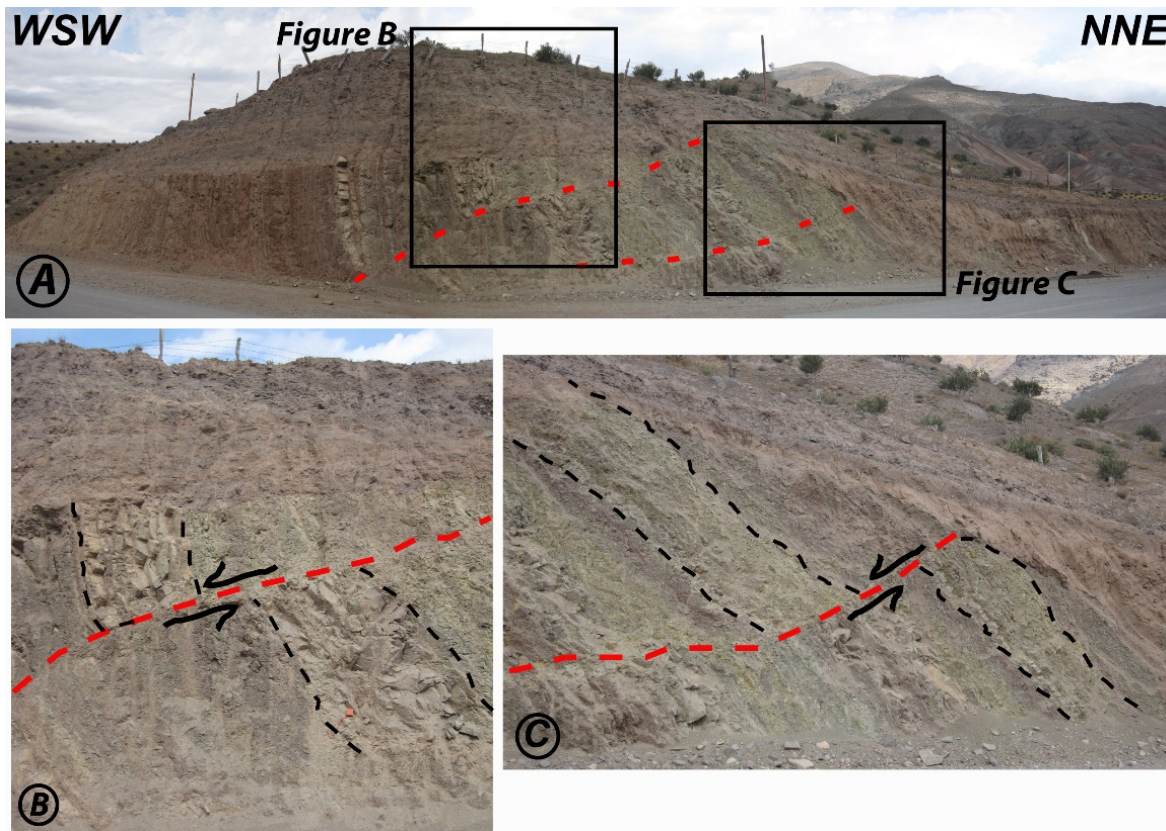


Figure 9. Apparent left-lateral displacement of clay stone, marl (green), siltstone and sandstone along active parallel fault segments in a site situated in front of Manjil dam. Black rectangles are enlarged in Figs. B and C to show the displacement.

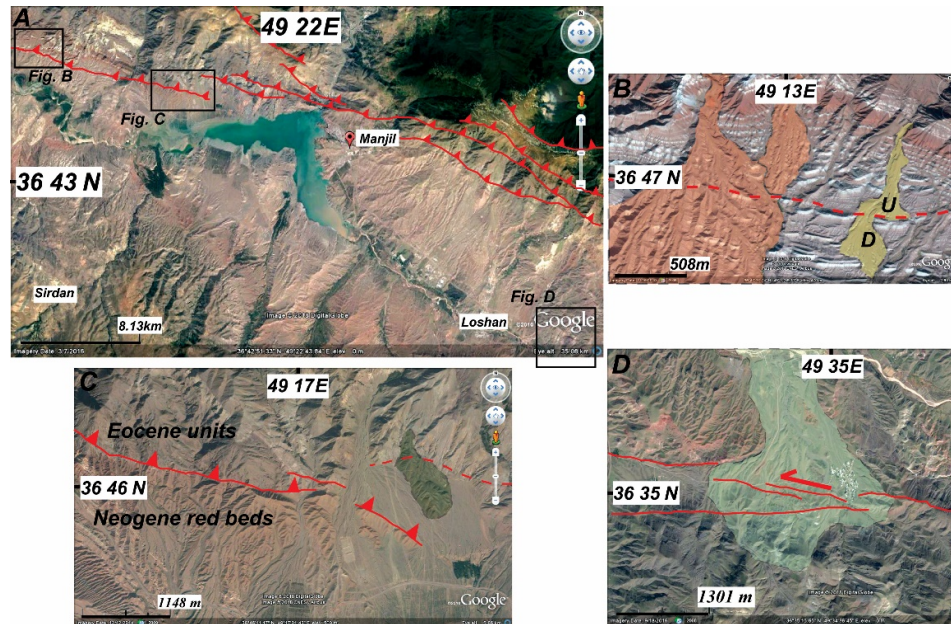


Figure 10. A. Satellite image of Manjil thrust fault beside Manjil dam and active faults affecting Quaternary units. B. Vertical uplift can be observed in a Quaternary alluvial fan. C. Thrust fault running between Eocene units and Neogene red beds in west of Aliabad. D. Left-lateral strike-slip fault movement recorded in a Quaternary alluvial fan situated in east of Loshan.

Fatalak village was completely ruined due to huge rock avalanche and all its 120 inhabitants were killed. Four other villages in Eshkevar region were also damaged severely by landslides and rockfalls. Based on previous studies (Ishihara *et al.*, 1992; Yegian *et al.*, 1995a, 1995b) widespread liquefaction and fissures at ground surface highly increased building damage mostly in villages, some located ~85km far from epicenter of the earthquake. Shabanzadeh *et al.* (2011) indicated that slope aspect and land use were the most important factors in occurrence of landslides in Deylaman region. Mahdaviyar & Memarian (2013) analyzed assessment of earthquake induced landslides triggered by Manjil-Rudbar earthquake in Rostamabad using knowledge-based hazard approach. Recent examples of seismic-induced landslides include numerous landslides triggered by this earthquake and also rock-falls induced by 2004 Baladeh earthquake (Tatar *et al.*, 2007).

Earthquake focal mechanisms indicate both high-angle reverse faulting and left-lateral strike-slip faulting mechanisms in high Alborz (Jackson *et al.*, 2002; Tatar & Hatzfeld, 2009; Berberian & Walker, 2010). Estimated values of stress drops for northern Iranian earthquakes contain higher mean value (Zafarani *et al.*, 2012) in comparison with low value for Zagros region. This fact is expected since most of northern Iranian seismic data consist of

midplate earthquakes, which generally occurred more than 500km far from plate margins (Zafrani & Mousavi, 2014). Rastgoo *et al.* (2018) reported low-velocity density feature in 50-100km depth range under western and central Alborz. They suggested that this anomaly may imply a mature delamination process event in western Alborz. Motaghi *et al.* (2010) conducted a study on microseismicity of northern Iran. Local recurrence time map was generated using microseismicity data during the period between 01/01/1996 to 05/15/2004. According to their results, one of three obtained anomalous areas that are interpreted as main asperities of the region is consistent with location of Baladeh earthquake on May 28, 2004. Berberian & Walker (2010) indicated that Manjil thrust fault was probably reactivated during Charazeh earthquake (Mw 5.4) on July 22, 1983. Sarkarinejad & Ansari (2015) suggested that Charazeh earthquake did not encourage Kelishom and Kashachal faults and also it did not trigger Rudbar destructive seismic event.

Salamat *et al.* (2017) calculated confidence intervals for maximum magnitude of earthquakes in different seismotectonic zones of Iran. Hashemi *et al.* (2017) presented a GIS-based time-dependent seismic source modeling for northern Iran. Nemati (2015) indicated 1990 Manjil-Rudbar and 1962 Buin-Zahra destructive earthquakes as the strongest

instrumentally recorded events in Alborz and its southern regions while higher geodetic slip rates implied shorter recurrence interval for large earthquakes on Rudbar Fault. According to his studies, area surrounding Manjil-Rudbar earthquake surface rupture is poorly covered by GPS stations and few GPS measurements indicate fault parallel surface velocity of 1.62 ± 0.6 mmyr⁻¹. It should be noted that a 6-year earthquake quiescence significantly occurred in Alborz range between 1971 and 1978 at middle of high rate interval. Seismic data analysis reflects high seismicity of western Alborz (e.g. Tatar & Hatzfeld, 2009; Barzegari *et al.*, 2017). No precise geochronologic data has been available for assessment of tectonic activities in this region. Barzegari *et al.* (2017) conducted a study on paleoseismology of Astara fault system. They concluded that moment magnitudes based on total offsets are estimated to range between 6.7-7.2 Mw. Considering the fact that recent low rate of seismicity in Alborz has been extended to 22 years, Nemati (2015) concluded that a partially quiet period approaches its end and a period of high seismic activity may start during next decades.

The Alborz mountain belt accommodates part of the differential motion between Central Iranian block and SCB. Jackson *et al.* (2002) estimated present motion of SCB to be $\sim 8-10$ mmyr⁻¹ to NW with respect to Eurasia. Axen *et al.* (2001) proposed that this motion may have begun in Pliocene. Jackson *et al.* (2002) suggested that rates and total cumulative slip of range-parallel left-lateral strike-slip in western Alborz are lower than those in east. SCB motion relative to Eurasia is calculated up to ~ 7 mmyr⁻¹ at an azimuth of 317°N (Mousavi *et al.*, 2013) based on GPS constraints on present-day deformation distribution in NE Iran. Djamour *et al.* (2010) considered a rigid body rotation as a significant factor affecting slip rates calculated for fault zones surrounding SCB block. Geodetic data (Walters *et al.*, 2013) indicated that SCB motion is likely to have a clockwise rotation relative to Eurasia about a pole much further away from the one calculated before. Paleomagnetic data (Cifelli *et al.*, 2015) suggested that Cretaceous volcanic rocks from western Alborz are characterized by clockwise rotation.

Arabia-Eurasia plate convergence has led to complex features in Iranian crust (Motaghi *et al.*, 2014) and lithospheric mantle (e.g. Mouthereau *et al.*, 2012). Motaghi *et al.* (2014) proposed that

Arabia and Eurasia lithosphere plates are under-thrust beneath Central Iran. Kadirov & Gadirov (2014) suggested that geodynamics of eastern Greater Caucasus collision zone has probably influenced orientation of SCB subduction zone (Abdollahzadeh *et al.*, 2014). SCB seems to have motion relative to both Eurasia and Central Iran accommodated by deformation at major boundaries along Ashkhabad (Mousavi *et al.*, 2013) and Shahrud (Hollingsworth *et al.*, 2008, Javidfakhr *et al.*, 2011) fault systems. Adjacent SCB westward motion with respect to Iran and consequently dominant left-lateral strike-slip movements in Alborz range are suggested to be initiated at ~ 10 Ma (Hollingsworth *et al.*, 2008); 5 ± 2 Ma (Axen *et al.*, 2001) and ~ 1.8 Ma (Ritz *et al.*, 2006). Based on previous studies (Guest *et al.*, 2006, 2007a, 2007b; Ballato *et al.*, 2008; Rezaeian *et al.*, 2012) contraction deformation in Alborz mountains probably occurred in incident rhythmic patterns while last one was at 5 ± 2 Ma (Allen *et al.*, 2011). This last incident is thought to reveal plate tectonic reconstruction of Arabia-Eurasia collision zone. A synchronous regional deformation initiated about 30-23 Ma considering distribution of cooling ages in margins of Iranian Plateau (Madanipour *et al.*, 2013). Northward trend change of compressional stress field led to exhumation along regional reverse northern and southern Talesh faults while a dominant strike-slip regime was established in central Talesh Mountains (Barzegari *et al.*, 2016; 2017; Madanipour *et al.*, 2017).

Interaction of faults or their segments in tectonically active regions can be observed on various temporal scales. The inversion tectonics in central Alborz was suggested by Zanchi *et al.* (2006). A NE transpressional tectonic regime (e.g. Ritz *et al.*, 2006) is active in Alborz range caused by N-S convergence of Central Iran together with SW motion of SCB toward Central Iran. Modern stress direction of $\sim N20^\circ E$ in Alborz Mountains (Masson *et al.*, 2007) results from integration of northward movement of Iranian Plateau/Central Iran and NW motion of SCB. Based on stress state reconstructions, Zamani & Masson (2014) suggested that E-Azarbaijan is colliding with SCB and Lesser Caucasus due to compressional stress and with Central Iranian Block and western Alborz due to strike-slip stress.

Quaternary deposits are widespread in southern plains of SCB. They are preserved in Qezel-Uzan valley and surrounding basins. Sedimentation

phases continued in the basins during Neogene and Quaternary. Parallel fault valleys represent fault activity in this area (Fig. 11). They triggered erosion and river captures that formed the present-day drainage pattern in a site close to Tashvir village (Fig. 11C). There are systematic parallel fault valleys surrounding Tashvir region. Most of fault plane data indicate strike-slip movements in this site (Fig. 11B). Fig. 12E shows another measurement site in vicinity of Tashvir village. Measured fault planes, fault steps and striations represent dominant left-lateral strike-slip movement.

Northeast of Loshan comprise several parallel strike-slip faults (Fig. 13A). The stereogram (Fig. 13C) indicates dominant strike-slip faults with minor component of normal faulting for the kinematic measurement site presented in Fig. 13A. Recent travertine deposits in Pakdeh and Sangrud regions are developed along major Quaternary active faults. There is a high topography region shown in Fig. 13D situated in north of Sangrud. The image presented in Fig. 13B illustrates rivers and rock layers of this mountainous area in a simple

schematic pattern. The mountains are in neighbourhood of a deep valley and this sharp elevation change is representative for the fault activity. Activity of the faults particularly the ones situated close to fault valley, can considerably motivate occurring landslides. Another fault trace is extended in northern parts of Loshan as presented in Fig. 13E. There are data available from kinematic measurements complemented by field observations. Kinematic inversion results determined by inversion method (Carey, 1979) are presented in Figs. 11C and 13B. The direction of present-day horizontal maximum stress axis (σ_1) is northeast-southwest considering kinematic measurements.

Shirin-Sou region is situated in south of Loshan. This area has a rugged high topography similar to other parts of Alborz Mountains. The steep elevations in this region are in proximity to deep valleys. Major heights and valleys are generally NE trending. Figs. 14 and 15 indicate oblique reverse motion in the sites situated close to Shirin-Sou village. Fig. 16B presents rough topography of the region which is related to location of reverse fault segments in Chahar Mahal region..

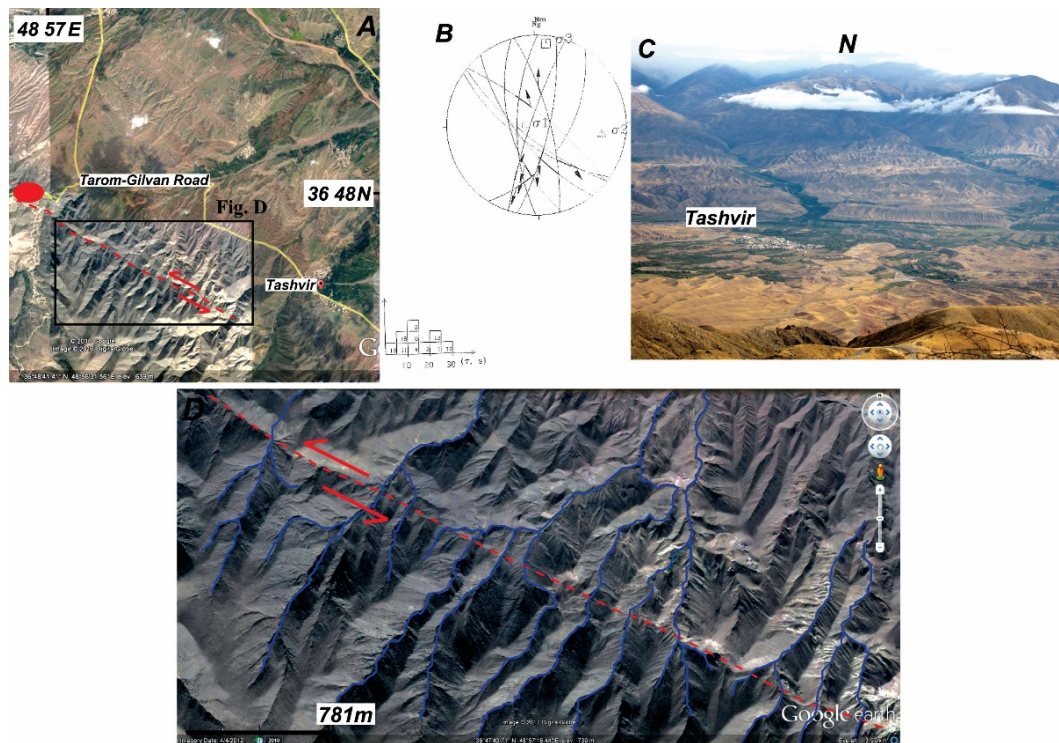


Figure 11. A. Satellite image of Tashvir-Gilvan road and kinematic measurement site which is shown by a red ellipse situated beside the road at left part of image. Left-lateral offsets along fault trace cut active streams. B. Lower hemisphere stereographic projections of fault plane data together with inversion results determined by inversion method (Carey, 1979). C. Tashvir village is shown in this photo. Parallel valleys are evidence for fault activity. D. The rectangle in Fig. A is enlarged in this image presenting left-lateral movement of the streams along the fault.

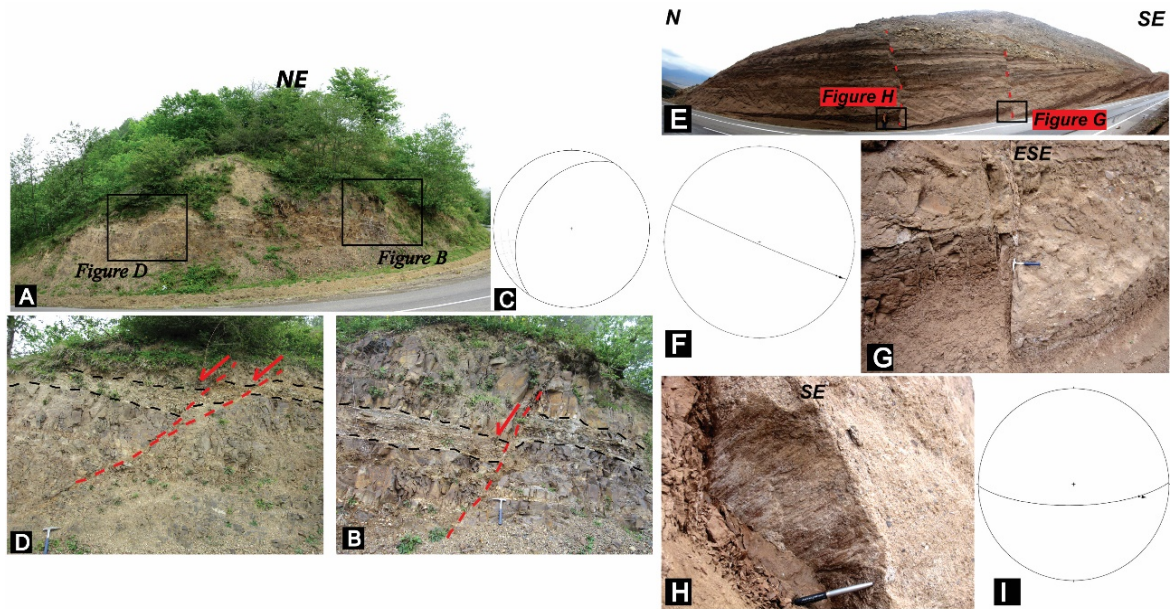


Figure 12. A. This site is located in vicinity of Deylaman village. Figs. B and D represent layer displacement. C. Fault plane presented in Fig. B is measured and lower hemisphere stereographic projection is given here. E. This site is situated in vicinity of Tashvir village. G. Geometry of fault plane is presented in a larger scale. Fig. H. Fault steps and striations measured on the fault plane are presented. F-I. Lower hemisphere stereographic projection for fault plane data.

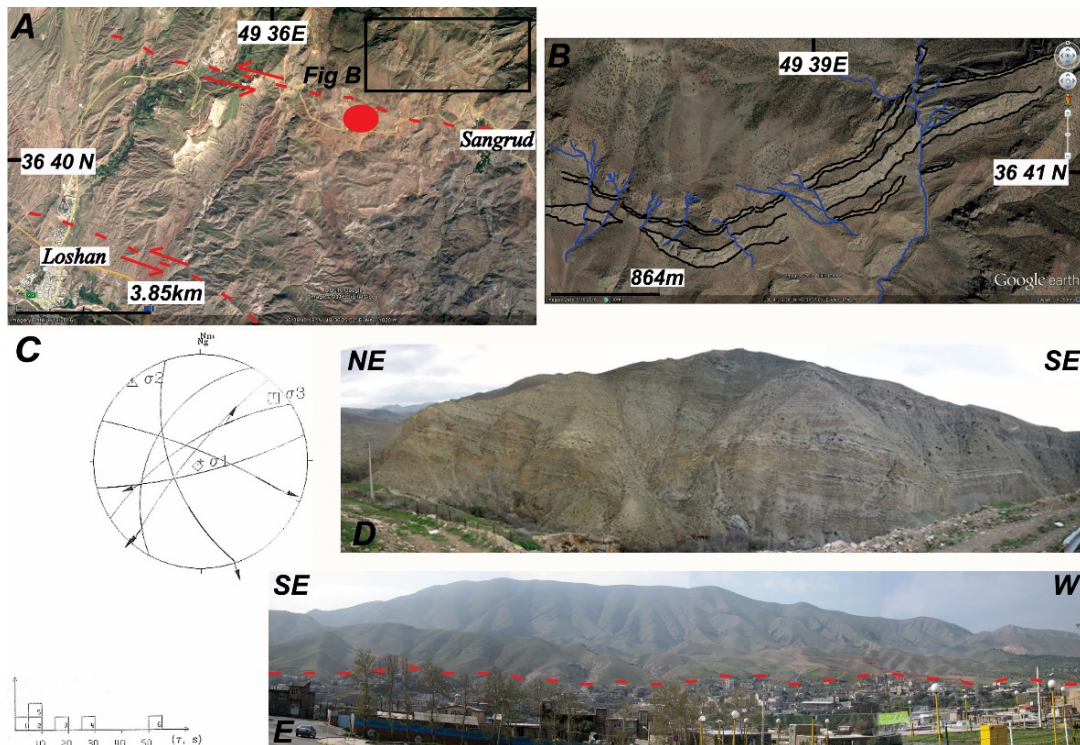


Figure 13. A. Kinematic measurement site beside Abhar-Loshan road is presented. B. The rectangle in Fig. A (north of Sangrud) is enlarged. The rivers and rock layers are shown in a simple schematic pattern. C. Lower hemisphere stereographic projections of fault plane data together with inversion results. D. Panoramic view of the mentioned site presented in Fig. B which is situated in NW of Sangrud village. E. The fault trace passing Loshan is shown in this landscape.

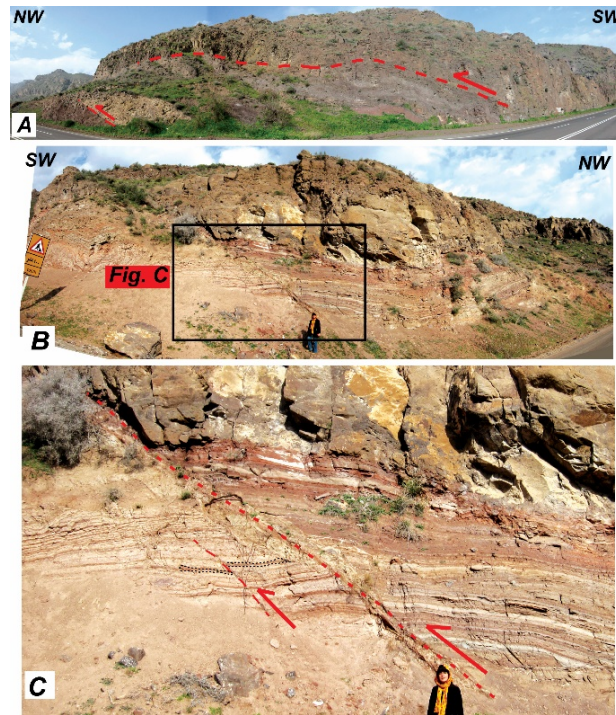


Figure 14. Thrust fault running between Eocene units and Neogene red beds in the outcrop found in Shirin-Sou to Loshan road. Figs B and C. represent reverse fault affecting Quaternary units in vicinity of Shirin-Sou village.

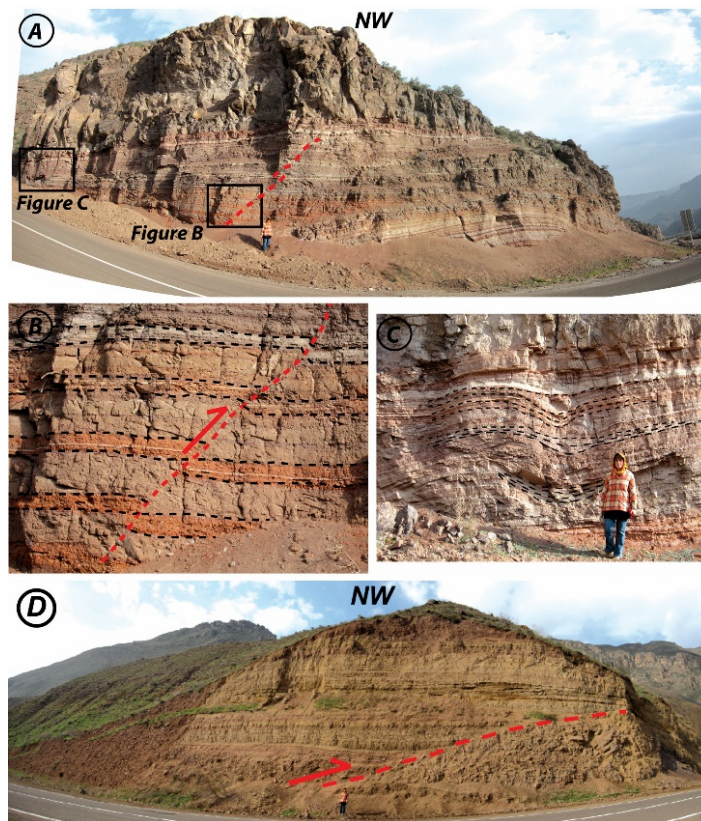


Figure 15. A. This site is situated close to Shirin-Sou village. B. Apparent offset of marl and gypsum units along active fault is enlarged in this image. The red key bed shows movement of the fault. C. Initial phase of folding growth in the layers due to compressional forces is shown in this image. D. Active thrust fault in Quaternary marl units located in vicinity of Shirin-Sou village.

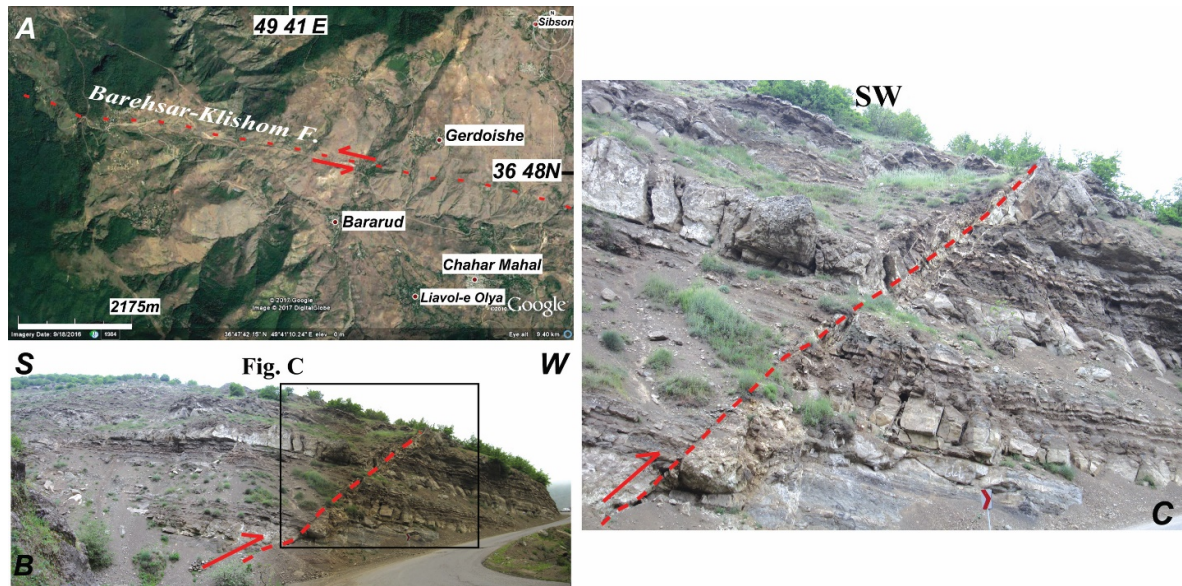


Figure 16. A. Left-lateral strike-slip Barehsar-Kelishom fault in north of Bararud and Chahr Mahal region. B-C. Oblique-reverse movement of the fault observed in a site situated in vicinity of Chahr Mahal.

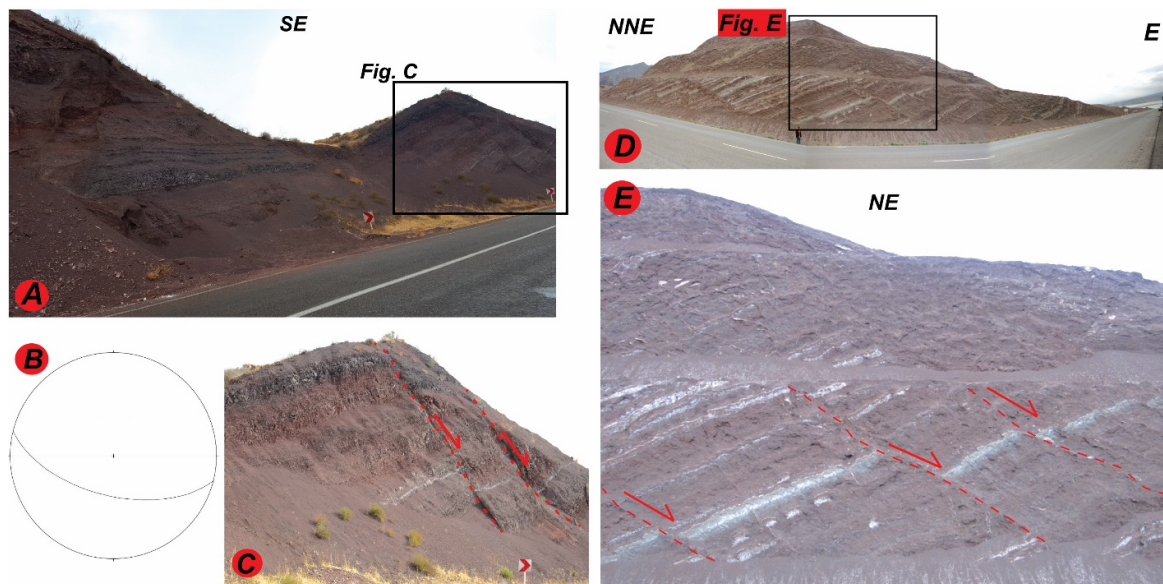


Figure 17. A. The image represents normal faulting in a site situated in major Taham-Tarom road. B. Lower hemisphere stereographic projection of fault plane data C. Displacement along normal fault is observed in this photo. D. Normal faulting in vicinity of Manjil dam. E. White key bed which is displaced along the fault.

Large areas of landslides particularly near Kelishom and Bareh-Sar villages (along Kelishom fault trace) could be associated with past high-magnitude earthquakes, which might not have necessarily occurred on Kelishom fault. Two examples of normal faulting in the area are presented in Taham-Tarom road (Fig. 17A) and in vicinity of Manjil dam (Fig. 17D).

Tatar & Hatzfeld (2009) analyzed microseismic evidence of slip partitioning for Manjil-Rudbar

earthquake. Considering different cross-sections, they concluded that a mixture of reverse and strike-slip faulting is resulted. They recognized a barrier between Kebateh and Zardgoli segments situated at Sefidrud River which did not experience surface deformation during the main shock. Berberian & Walker (2010) studied Manjil-Rudbar earthquake and its aftershocks together with active faulting in a more extended region. We provided a more detailed view of active tectonics in this fault zone,

concentrating on geomorphic and Pliocene-Quaternary geologic evidence. Earthquake focal mechanism for the earthquake which occurred on December 3, 1980 (Fig. 1 and Table 1, Mw 5.3) is considerably similar with Manjil-Rudbar earthquake focal mechanism. The mentioned seismic event (Fig. 1, ID number 2) occurred in southern border of SCB. High similarity exists for the earthquakes which occurred in south of Talesh (Fig. 1, ID number 1, Mw 6.3) and northeast of Talesh (Fig. 1, ID number 10, Mw 6.5). Masouleh fault probably was responsible for the seismic event which occurred on April 11, 1978 (Table 1, ID number 1). Fault plane solutions generally indicate a radial pattern of thrusting in western Alborz. Alborz Mountains comprises structural heterogeneities inherited from different tectonic events. The fault segments in the study region are arranged in oblique left-lateral and reverse fault zones which represent active compressional strike-slip movements in western Alborz resulting structural complexities in this region.

The data presented in this article can resolve tectonic activity of Manjil-Rudbar fault zone; characterizing western Alborz regional tectonic framework. This paper confirms significance of geomorphic considerations for understanding tectonic activities in this seismic zone. The fault

zone is composed of generally NW trending fault segments extended along southwestern boundary of SCB affecting Quaternary deposits. Major fault segments were mapped in order to recognize structural and geomorphic features of the fault zone. Satellite images were used to improve the visualization of fault traces in order to constrain their geometry considering structural linkage between different fault segments. Major geomorphic features in the study area provide good schematic pattern to understand how changes in kinematic regime affected the region. Manjil Thrust fault marks a distinct topographic boundary between mountainous regions and Quaternary basins. Left-lateral strike-slip and thrust movements were observed all over Manjil-Rudbar fault zone corresponding to recent fault activities of Rudbar, Manjil, Kelishom and Jirandeh (Kashachal) faults. The faults are supported by field geologic data and kinematic measurements. Left-lateral displacements on nearby Kelishom, Kashachal and other parallel fault segments in the region define them eastward continuations of Manjil-Rudbar fault zone. These segments may cause severe seismic events in this region in future. We discussed seismic-induced hazards in Manjil-Rudbar earthquake. The results are useful to establish history of regional deformation in this seismic area of northern Iran.

References

- Abdollahzadeh, G.h., Sajjini, M., Shahaky, M., Zahedi Tajrishi, F., Khanmohammadi, L., 2014. Considering potential seismic sources in earthquake hazard assessment for Northern Iran. *Journal of Seismology*, 18: 357–369.
- Allen, M., Jackson, J., Walker, R., 2004. Late Cenozoic reorganization of the Arabia-Eurasia collision and the comparison of short-term and long term deformation rates. *Tectonics*, 23: 1-16.
- Allen, M.B., M. Kheirkhah, M.H. Emami, Jones, S.J., 2011. Right-lateral shear across Iran and kinematic change in the Arabia-Eurasia collision zone. *Geophysical Journal International*, 184 (2): 555–574.
- Ambraseys, N., Melville, C.P., 1982. *History of Persian earthquakes*. Cambridge University Press, UK, 219 pages.
- Ambraseys, N., Moinfar, A., 1973. The seismicity of Iran. The Firuzabad (Nehavend) earthquake of 16 August 1958. *Imperial College of Science, London*, 27: 1-21.
- Ashtari Jafari, M., 2016. *Lessons Learned from the Recent Earthquakes in Iran*. Springer Natural Hazards book series, Earthquakes and Their Impact on Society, p 459-474.
- Audemard, F.A., 2003. Geomorphic and geologic evidence of ongoing uplift and deformation in the Merida Andes, Venezuela. *Quaternary International* (101–102): 43–65.
- Axen, G.J., Lam, P.S., Grove, M., Stockli, D.F., Hassanzadeh, J., 2001. Exhumation of the west-central Alborz Mountains, Iran, Caspian subsidence, and collision-related tectonics. *Geology*, 29 (6): 559–562.
- Aziz Zanjani, A., Ghods, A., Sobouti, F., Bergman, E., Mortezaejad, G.H., Priestly, K., Madanipour, S., Rezaeian, M., 2013. Seismicity in the western coast of the South Caspian Basin and the Talesh Mountains. *Geophysical Journal International*, 195 (2): 799-814.
- Ballato, P., Nowaczyk, N.R., Landgraf, A., Strecker, M.R., Friedrich, A., Tabatabaei, S.H., 2008. Tectonic control on sedimentary facies pattern and sediment accumulation rates in the Miocene foreland basin of the southern Alborz mountains, northern Iran. *Tectonics*, 27 (6): 1-20.
- Ballato, P., Stockli, D.F., Ghassemi, M.R., Landgraf, A., Strecker, M.R., Hassanzadeh, J., Friedrich, A., Tabatabaei, S.H., 2013. Accommodation of transpressional strain in the Arabia-Eurasia collision zone: new constraints from (U-Th)/He thermochronology in the Alborz mountains, north Iran. *Tectonics*, 32: 1–18.
- Ballato, P., Landgraf, A., Schildgen, T.F., Stockli, D. F., Fox, M., Ghassemi, M.R., Kirby, E., Strecker, M.R., 2015. The

- growth of a mountain belt forced by base-level fall: Tectonics and surface processes during the evolution of the Alborz Mountains, N Iran. *Earth and Planetary Science Letters*, 425: 204–218.
- Barzegari, A., Esmaili, R., Ebrahimi, M., Faghih, A., Ghorashi, M., Nazari, H., 2016. Evaluation of Slip Rate on Astarra Fault System, North Iran. *Journal of Earth Science*, 27 (6): 971–980.
- Barzegari, A., Ghorashi, M., Nazari, H., Fontugne, M., Shokri, M.A., Pourkermani, M., 2017. Paleoseismological Analysis along the Astarra Fault System (Talesh Mounatins, North Iran). *Acta Geologica Sinica*, 91 (5): 1553-1572.
- Bastami, M., Soghrat, M.R., 2017. An empirical method to estimate fatalities caused by earthquakes: the case of the Ahar–Varzaghan earthquakes (Iran). *Natural Hazards*, 86: 125–149.
- Bastaminia, A., Rezaei, M.R., Dastoorpoor, M., 2017. Identification and evaluation of the components and factors affecting social and economic resilience in city of Rudbar, Iran. *International Journal of Disaster Risk Reduction*, 22: 269-280.
- Berberian, M., 1983. The southern Caspian: a compressional depression floored by a trapped, modified oceanic crust. *Canadian Journal of Earth Sciences*, 20: 163–183.
- Berberian, M., Qorashi, M., Jackson, J.A., Priestley, K., Wallace, T., 1992. The Rudbar-Masson earthquake of 20 June 1990 in NW Persia: preliminary field and seismological observations, and its tectonic significance. *Bulletin of the Seismological Society of Americ*, 82 (4): 1726–1755.
- Berberian, M., Walker, R., 2010. The Rudbar Mw 7.3 earthquake of 1990 June 20; seismotectonics, coseismic and geomorphic displacements, and historic earthquakes of the western ‘High-Alborz’, Iran. *Geophysical Journal International*, 182: 1577–1602.
- Berberian, M., 2014. Earthquake and Coseismic Surface Faulting on the Iranian Plateau, a historical, social and physical approach. Elsevier B.V (Ed.), Netherlands, volume 17, 776 pages.
- Cifelli, F., Ballato, P., Alimohammadian, H., Sabouri, J., Mattei, M., 2015. Tectonic magnetic lineation and oroclinal bending of the Alborz Range: implications on the Iran-southern Caspian Geodynamics. *Tectonics*, 34 (1): 116–132.
- Carey, E., 1979. Recherche des directions principales de contraintes associées au jeu d'une population de failles. *Revue Géographie Physique Geologie Dynamique*, 21: 57–66.
- Djamour, Y., Vernant, P., Bayer, R., Nankali, H.R., Ritz, J.F., Hinderer, J., Hatam, Y., Luck, B., Le Moigne, N., Sedighi, M., Khorrani, F., 2010. GPS and gravity constraints on continental deformation in the Alborz Mountain range, Iran. *Geophysical Journal International*, 183: 1287-1301.
- Djamour, Y., Vernant, P., Nankali, H.R., Tavakoli, F., 2011. NW Iran-eastern Turkey present-day kinematics: Results from the Iranian permanent GPS network. *Earth and Planetary Science Letters*, 307 (1-2): 27–34.
- Fatemi Aghda, S.M., Ghayoumian, J., Suzuki, A., Kitazono, Y., Nogole Sadat, A.A., 1992. Evaluation of effective factors causing ground failures during 1990 Manjil-Iran earthquake. *Proceedings Symposium, Bangkok (Ed.)*, 327-339.
- Gao, L., and Wallace, T.C., 1995. The 1990 Rudbar-Tarom Iranian earthquake sequence: Evidence for slip partitioning. *Journal of Geophysical Research*, 100 (B8): 15317–15332.
- Guest, B., Stockli, D.F., Grove, M., Axen, G.J., Lam, P.S, Hassanzadeh, J., 2006. Thermal histories from the central Alborz mountains, northern Iran: implications for the spatial and temporal distribution of deformation in northern Iran. *Geological Society of American Bulletin*, 118: 1507-1521.
- Guest, B., Guest, A., Axen, G., 2007a. Late Tertiary tectonic evolution of northern Iran: A case for simple crustal folding. *Global and Planetary Change*, 58 (1-4): 435–453.
- Guest, B., Horton, B.K., Axen, G.J., Hassanzadeh, J., McIntosh, W.C., 2007b. Middle to late Cenozoic basin evolution in the western Alborz Mountains: Implications for the onset of collisional deformation in northern Iran. *Tectonics*, 26 (6): 1-26.
- Hakimi Asiabar, S., Bagheriyan, S., 2017. Exhumation of the Deylaman fault trend and its effects on the deformation style of the western Alborz belt in Iran. *International Journal of Earth Sciences*, 107 (2): 539-551.
- Hamzehloo, H., Sarkar, I., Chander, R., 1997. Analysis of some aftershocks of the Rudbar earthquake of 1990 using master event technique. *Bulletin of the Indian Society of Earthquake Technology*, 33: 1–16.
- Hashemi, M., Alesheikh, A.A., Zolfaghari, M.R., 2017. A GIS-based time-dependent seismic source modeling of Northern Iran. *Earthq Engineering and Engineering Vibration*, 16: 33-45.
- Hollingsworth, J., Jackson, J., Walker, R., Nazari, H., 2008. Extrusion tectonics and subduction in the eastern South Caspian region since 10 Ma. *Geology*, 36 (10): 763–766.
- Ibrion, M., Mokhtari, M., Nadim, F., 2015. Earthquake Disaster Risk Reduction in Iran: Lessons and ‘‘Lessons Learned’’ from Three Large Earthquake Disasters-Tabas 1978, Rudbar 1990, and Bam 2003. *International Journal of Disaster Risk Science*, 6: 415–427.
- Ishihara, K., Haeri, S.M., Moinfar, A.A., Towhata, I., Tsujino, S., 1992. Geotechnical aspects of the June 20, 1990 Manjil earthquake in Iran. *Soils and Foundations*, 32 (3): 61-78.
- Jackson, J., Priestley, K., Allen, M., Berberian, M., 2002. Active tectonics of the South Caspian Basin. *Geophysical Journal International*, 148: 214–245.

- Jafari, M.K., Montazer, S., Heydari, M., 2000. Earthquake triggered landslide studies in Alborz. International Institute of Earthquake Engineering and Seismology, Tehran, Iran.
- Javidfakhr, B., Bellier, O., Shabanian, E., Siame, L., Léanni, L., Boulrès, D., Ahmadian, S., 2011. Fault kinematics and active tectonics at the southeastern boundary of the eastern Alborz (Abr and Khij fault zones): geodynamic implications for NNE Iran. *Journal of Geodynamics*, 52: 290–303.
- Kadirov, F.A., Gadirov, A.H., 2014. A gravity model of the deep structure of South Caspian Basin along submeridional profile Alborz–Absheron Sill. *Global and Planetary Change*, 114: 66–74.
- Khodaverdian, A., Zafarani, H., Rahimian, M., 2015. Long term fault slip rates, distributed deformation rates and forecast of seismicity in the Iranian Plateau. *Tectonics*, 34: 2190–2220.
- Kurtz, R., Klinger, Y., Ferry, M., Ritz, J-F., 2018. Horizontal surface-slip distribution through several seismic cycles: The Eastern Bogd fault, Gobi-Altai, Mongolia. *Tectonophysics (734-735)*: 167-182.
- Madanipour, S., Ehlers, T.A., Yassaghi, A., Rezaeian, M., Enkelmann, E., Bahroudi, A., 2013. Synchronous Deformation on orogenic plateau margins, insights from the Arabia-Eurasia collision, *Tectonophysics*, (608): 440-451.
- Madanipour, S., Yassaghi, A., Ehlers, T.A., Enkelmann, E., 2017. Accelerated middle Miocene exhumation of the Talesh Mountains constrained by U-Th/He thermochronometry: evidence for the Arabia-Eurasia collision in the NW Iranian Plateau. *Tectonics*, 36 (8): 1538–1561.
- Mahdavi, M.R., Memarian, P., 2013. Assessment of earthquake induced landslides triggered by Roudbar–Manjil earthquake in Rostamabad (Iran) quadrangle using knowledge-based hazard analysis approach. In: Ugai K, Yagi H, Wakai A (Eds) *Earthquake-induced landslides*. Springer, Berlin, 769–780.
- Masson, F., Anvari, M., Djamour, Y., Walpersdorf, A., Tavakoli, F., Daignières, M., Nankali, H., Van Gorp, S., 2007. Large-scale velocity field and strain tensor in Iran inferred from GPS measurements: new insight for the present-day deformation pattern within NE Iran. *Geophysical Journal International*, 170: 436–440.
- Moinfar, A.A., Nader Zadeh, A., 1990. An Immediate and Preliminary Report on the Manjil Iran earthquake of 20 June 1990. Building and Housing research Center, Report Number 119.
- Motaghi, K., Hessami, K., Tatar, M., 2010. Pattern recognition of major asperities using local recurrence time in Alborz Mountains, Northern Iran. *Journal of Seismology*, 14 (4): 787–802.
- Motaghi, K., Tatar, M., Priestley, K., Romanelli, F., Doglioni, C., Panza, G.F., 2014. The deep structure of the Iranian Plateau. *Gondwana Research*, 28 (1): 407-418.
- Mousavi, Z., Walpersdorf, A., Walker, R.T., Tavakoli, F., Pathier, E., Nankali, H., Nilfouroushan, F., Djamour, Y., 2013. Global positioning system constraints on the active tectonics of NE Iran and the South Caspian region. *Earth and Planetary Science Letters (377-378)*: 287-298.
- Mouthereau, F., Lacombe, O., Vergès, J., 2012. Building the Zagros collisional orogen: Timing, strain distribution and the dynamics of Arabia/Eurasia plate convergence. *Tectonophysics (532-535)*: 27–60.
- Muttoni, G., Mattei, M., Balini, M., Zanchi, A., Gaetani, A., Berra, F., 2009. The drift history of Iran from the Ordovician to the Triassic. In: Geological Society of London, Special Publication: South Caspian to Central Iran Basins, 312: 7-29.
- National Geophysical Data Center, NOAA, 2016. National Geophysical Data Center/World Data Service (NGDC/WDS): Global Significant Earthquake Database. <http://www.ngdc.noaa>.
- Nazari, H., Salamati, R., 1998. Geological Quadrangle Map of Rudbar, scale 1: 100, 000, Geological Survey of Iran, Tehran.
- Nemati, M., 2015. Intermediate-term variations in 200 years seismicity at the north of Iran. *Journal of Seismology*, 19 (2): 585-605.
- Niazi, M., Bozorgnia, Y., 1992. The 1990 Manjil, Iran earthquake: geology and seismological overview, PGA attenuation and observed damage. *Bulletin of the Seismological Society of America*, 82: 774–799.
- Rastgoo, M., Rahimi, H., Motaghi, K., Shabanian, E., Romanelli, F., Panza, G. F., 2018. Deep structure of the Alborz Mountains by joint inversion of P receiver functions and dispersion curves. *Physics of the Earth and Planetary Interiors*, 277: 70–80.
- Reilinger, R., McClusky, S., Vernant, P., and 22 others, 2006. GPS constraints on continental deformation in the Africa–Arabia–Eurasia continental collision zone and implications for the dynamics of plate interactions. *Journal of Geophysical Research*, 111, B05411. doi:10.1029/2005JB004051.
- Rezaeian, M., Carter, A., Hovius, N., Allen, M.B., 2012. Cenozoic exhumation history of the Alborz Mountains, Iran: New constraints from low temperature chronometry. *Tectonics*, 31: 1-20.
- Ritz, J-F., Nazari, H., Ghassemi, A., Salamati, R., Shafei, A., Solaymani, S., Vernant, P., 2006. Active transtension inside Central Alborz: a new insight into northern Iran–southern Caspian geodynamics. *Geology*, 34 (6): 477–480.
- Robert, A.M., Letouzey, J., Kavooosi, M.A., Sherkati, S., Muller, C., Verges, J., Aghababaei, A., 2014. Structural evolution of the Kopeh Dagh fold-and-thrust belt (NE Iran) and interactions with the South Caspian Basin and Amu Darya Basin. *Marine and Petroleum Geology*, 57: 68-87.

- Salamat, M., Zare, M., Holschneider, M., Zoller, G., 2017. Calculation of Confidence Intervals for the Maximum Magnitude of Earthquakes in Different Seismotectonic Zones of Iran. *Pure and Applied Geophysics*, 174: 763–777.
- Sarkar, I., Hamzehloo, H., Khattri, K.N., 2003. Estimation of causative fault parameters of the Rudbar earthquake of June 20, 1990 from near field SH-wave data. *Tectonophysics*, 364: 55–70.
- Sarkarinejad, K., Ansari, S., 2015. Did the 1983 Charazeh earthquake trigger the destructive 1990 Rudbar earthquake? *International Journal of Earth Sciences*, 104 (1): 309–319.
- Shabanzadeh, K., Suroor, J., Mohammadi Torkashvand, A., 2011. Zoning Landslide by Use of Frequency Ratio Method (Case Study: Deylaman Region). *Middle-East Journal of Scientific Research*, 9 (5): 578–583.
- Sharma, G., Champati ray, P.K., Mohanty S., 2018. Morphotectonic analysis and GNSS observations for assessment of relative tectonic activity in Alaknanda basin of Garhwal Himalaya, India. *Geomorphology*, 301: 108–120.
- Tatar, M., Jackson, J., Hatzfeld, D., Bergman, E., 2007. The 2004 May 28 Baladeh Earthquake (Mw 6.2) in the Alborz, Iran: overthrusting the South Caspian Basin margin, partitioning of oblique convergence and the seismic hazard of Tehran. *Geophysical Journal International*, 170: 249–261.
- Tatar, M., Hatzfeld, D., 2009. Microseismic evidence of slip partitioning for the Rudbar-Tarom Earthquake (Ms 7.7) of 1990 June 20 in NW Iran. *Geophysical Journal International*, 176: 529–541.
- VahidiFard, H., Zafarani, H., Sabbagh-Yazdi, S.R., Hadian, M.A., 2017. Seismic hazard analysis using simulated ground-motion time histories: The case of the Sefidrud dam, Iran. *Soil Dynamics and Earthquake Engineering*, 99: 20–34.
- Van der Boon, A., van Hinsbergen, D.J.J., Rezaeian, M., Gürer, D., Honarmand, M., Pastor-Galán, D., Krijgsman, W., Langereis, C.G., 2018. Quantifying Arabia–Eurasia convergence accommodated in the Greater Caucasus by paleomagnetic reconstruction. *Earth and Planetary Science Letters*, 482: 454–469.
- Vernant, P., Nilforoushan, F., Chéry, J., Bayer, R., Djamour, Y., Masson, F., Nankali, H., Ritz, J.-F., Sedighi, M., Tavakoli, F., 2004. Deciphering oblique shortening of central Alborz in Iran using geodetic data. *Earth and Planetary Science Letters*, 223: 177–185.
- Walters, R.J., Elliott, J.R., Li, Z., Parsons, B., 2013. Rapid strain accumulation on the Ashkabad fault (Turkmenistan) from atmosphere corrected InSAR. *Journal of Geophysical Research*, 118: 3674–3690.
- Yan, B., Lin, A., 2015. Systematic deflection and offset of the Yangtze River drainage system along the strike-slip Ganzi-Yushu-Xianshuihe Fault Zone, Tibetan Plateau. *Journal of Geodynamics*, 87: 13–25.
- Yegian, M.K., Ghahraman, V.G., Nogole-Sadat, M.A., Daraie, H., 1995a. Liquefaction during the 1990 Manjil, Iran, earthquake, I: Case history data. *Bulletin of the Seismological Society of America*, 85 (1): 66–82.
- Yegian, M.K., Ghahraman, V.G., Nogole-Sadat, M.A.A., Daraie, H., 1995b. Liquefaction during the 1990 Manjil, Iran, earthquake, II: Case history analyses. *Bulletin of the Seismological Society of America*, 85 (1): 83–92.
- Zafarani, H., Hassani, B., Ansari, A., 2012. Estimation of earthquake parameters in the Alborz seismic zone, Iran using generalized inversion method. *Soil Dynamics and Earthquake Engineering*, 42: 197–218.
- Zafarani, H., Mousavi, M., 2014. Applicability of different ground-motion prediction models for northern Iran. *Natural Hazards*, 73: 1199–1228.
- Zamani, B., Masson, F., 2014. Recent tectonics of East (Iranian) Azerbaijan from stress state reconstructions. *Tectonophysics*, 611: 61–82.
- Zanchi, A., Berra, F., Mattei, M., Ghassemi, M.R., Sabouri, J., 2006. Inversion tectonics in central Alborz, Iran. *Journal of Structural Geology*, 28: 2023–2037.
- Zolfaghari, M.R., 2009. Geodetic deformation vs. seismic strain deduced by historical earthquakes across the Alborz Mountains. *Journal of Seismology*, 13: 647–663.